

First experience using F-18-flubrobenguane PET imaging in patients with the suspicion of pheochromocytoma or paraganglioma

Lukas Kessler¹, Anna M. Schlitter², Markus Krönke³, Alexander von Werder⁴, Robert Tauber⁵, Tobias Maurer⁵, Simon Robinson⁶, Cesare Orlandi⁶, Michael Herz³, Behrooz H. Yousefi^{3,7}, Stephan G. Nekolla³, Markus Schwaiger³, Matthias Eiber^{*3}, Christoph Rischpler^{*1,3}

¹ Department of Nuclear Medicine, University Hospital Essen, University of Duisburg-Essen, Essen, Germany

² Institute of Pathology, Technical University Munich, Munich, Germany

³ Department of Nuclear Medicine, Klinikum rechts der Isar, Technical University of Munich, Munich,

⁴ Department of Gastroenterology, Klinikum rechts der Isar, Technical University of Munich, Munich, Germany

⁵ Department of Urology, Klinikum rechts der Isar, Technical University of Munich, Munich, Germany

⁶ Discovery Research, Lantheus Medical Imaging, North Billerica, Massachusetts

⁷ Department of Nuclear Medicine, Philipps University of Marburg. Marburg, Germany

*The two last authors contributed equally to the work.

Corresponding author:

Christoph Rischpler, MD

Email: C.Rischpler@tum.de

Phone: +49 (0) 89 /4140-6085

Klinikum rechts der Isar,

Nuklearmedizinische Klinik und Poliklinik

Ismaninger Str. 22

81675 München

First author:

Lukas Kessler, MD

Email: Lukas.Kessler@uk-essen.de

Phone: +49 (0) 201 723 83297

Universitätsklinikum Essen

Klinik für Nuklearmedizin

Hufelandstrasse 55

45147 Essen

Word count: 4820

Short running title: F-18-flubrobenguane PET in PHEO or PGL

ABSTRACT

Rationale: Pheochromocytomas and paragangliomas are a rare tumor entity originating from adreno-medullary chromaffin cells in the adrenal medulla or in sympathetic, paravertebral ganglia outside the medulla. Especially small lesions are difficult to detect by conventional CT or MR imaging and even by SPECT imaging with currently available radiotracers (e.g. MIBG). The novel PET-radiotracer F-18-flubrobenguane could change the diagnostic paradigm in suspected pheochromocytomas and paragangliomas due to its homology to MIBG and the general advantages of PET-imaging. Aim of this retrospective analysis was to evaluate F-18-flubrobenguane in pheochromocytomas and paragangliomas and to investigate the biodistribution in patients.

Methods: 24 Patients with suspected pheochromocytoma and paraganglioma underwent PET/CT or PET/MRI at 63 ± 24 min p.i. after injection of 256 ± 33 MBq F-18-flubrobenguane. SUV_{mean} and SUV_{max} values of organs were measured with spherical volume-of-interests. Threshold segmented volume-of-interests were used to measure $SUV_{\text{mean/max}}$ of the tumor lesions. One reader evaluated all cross-sectional imaging datasets (CT or MRI) separately as well as the PET hybrid datasets and reported lesion number and size. A three point-scale indicating the diagnostic certainty for a positive lesion was assigned.

Results: F-18-flubrobenguane showed a reproducible, stable biodistribution with highest values of $SUV_{\text{max/mean}}$ in the thyroid gland ($30.3 \pm 2.2 / 22.5 \pm 1.6$), pancreas ($12.2 \pm 0.8 / 9.5 \pm 0.7$), tumor lesions ($16.8 \pm 1.7 / 10.1 \pm 1.1$) and the lowest $SUV_{\text{max/mean}}$ values in muscle ($1.1 \pm 0.06 / 0.7 \pm 0.04$) and lung ($2.5 \pm 0.17 / 1.85 \pm 0.13$). In a subgroup analysis both pheochromocytoma and paraganglioma lesions showed a significantly higher average SUV_{mean} compared to healthy adrenal glands (11.9 ± 2.0 vs 9.9 ± 1.5 vs 3.7 ± 0.2). In total 47 lesions were detected. The reader reported more and smaller lesions with higher certainty in PET hybrid imaging compared to conventional imaging, however, statistical significance was not

reached. 61% (14/23) of the 23 (23/47, 49%) lesions smaller than 1 cm were found on hybrid imaging only.

Conclusion: Our preliminary data suggest F-18-flubrobenguane PET as a new effective staging tool in patients with suspected pheochromocytoma and paraganglioma. Major advantages are the fast acquisition and high spatial resolution of PET imaging and intense uptake in tumor lesions facilitating lesion detection. Further studies are warranted to define its role particularly in comparison to standard diagnostic procedures such as MRI or I-123-MIBG SPECT/CT.

Pheochromocytomas are rare, catecholamine-producing tumors originating from adreno-medullary chromaffin cells in the adrenal medulla or in sympathetic, paravertebral ganglia outside the medulla (the latter are usually referred to as paragangliomas) (1,2). Sympathetic paragangliomas may be located in the pelvis, the abdomen or in the thorax. About 80-85% of pheochromocytomas arise from adrenal medulla, while 15-20% originate from extra-adrenal chromaffin tissue (1). Pheochromocytomas and paragangliomas may occur in the context of genetic disorders (3–5). Furthermore, pheochromocytomas may be bilateral in more than 10% or even multifocal (particularly in familial pheochromocytoma syndromes) (1,6). Malignancy in adrenal pheochromocytomas is relatively rare ($\leq 5\%$), but is quite common in paragangliomas with up to 33% (1,7). It is important to point out that there is no genetic or histological marker that definitely indicates malignancy in these tumors, being also the reason that malignancy is defined as the occurrence of metastasis in the WHO classification (8). Surgery is generally recommended as the primary treatment with curative intention (2). These facts illustrate the immense importance of preoperative non-invasive disease assessment.

CT is recommended as the primary imaging modality due to a high sensitivity of about 90%, while MRI is recommended in special situations only (e.g. paragangliomas of the head and neck, contrast media allergy, young patients) (2,9,10). Both CT and MRI suffer from low specificity. In contrast, iodine-labeled (I-123- or I-131) metaiodobenzylguanidine (MIBG) scintigraphy and SPECT imaging demonstrate a high specificity ranging from 70-100% at an acceptable sensitivity (56-88%) for both, pheochromocytomas and paragangliomas (2). However, PET imaging is usually preferred over SPECT due its higher sensitivity and higher spatial resolution often resulting in higher diagnostic accuracy (11). Also, PET allows for truly quantitative imaging facilitating response assessment (11) and has shorter acquisition times.

Available PET tracers for the assessment of pheochromocytomas or paragangliomas are F-18-fludeoxyglucose (FDG), somatostatin receptor targeting tracers such as Ga-68-DOTATATE and rarely-used PET-tracers like C-11-

hydroxyephedrine (mHED), F-18-fluoro-dopa, F-18-fluorodopamine or I-124 MIBG. However, these radiotracers suffer from disadvantages such as long half-life and high cost (I-124), the need for an onsite-cyclotron (C-11), a complex radiosynthesis (F-18 fluoro-dopa, F-18 fluorodopamine) or a low specificity for pheochromocytoma and paraganglioma (somatostatin receptor targeting tracers) (12–14). N-[3-bromo-4-(3-(18)F-fluoro-propoxy)-benzyl]-guanidine (F-18-flubrobenguane, formerly known as LMI1195) is a novel, F-18 labeled radiotracer which has a high homology to MIBG and can visualize norepinephrine-transporters with a high affinity and specificity (15). This radiotracer has been evaluated successfully in a MENX tumor model, a rat model with bilateral pheochromocytomas (16). In humans, this radiotracer has been evaluated in healthy volunteers for biodistribution and radiation dosimetry studies and in a recent case report of 74-year man with heart failure who received a F-18-flubrobenguane and C-11-mHED PET (17,18). The aim of this retrospective analysis was to evaluate F-18-flubrobenguane in patients with the suspicion of pheochromocytomas or paragangliomas.

MATERIALS AND METHODS

Radiotracer Synthesis

F-18-flubrobenguane was synthesized as previously described (15).

Briefly, the synthesis was performed using a brosylate precursor and one-step n.c.a F-18 displacement reaction with high-performance liquid chromatography purification. Radiochemical purity was at least 95% in all performed synthesis and specificity was >130 GBq/μmol. The radiotracer was formulated in an 8% ethanol/saline solution.

All patients gave written informed consent for the procedure as a legal requirement for F-18-flubrobenguane PET/CT or PET/MR imaging on a compassionate use basis. All reported investigations were conducted in accordance with the Helsinki Declaration and with national regulations. The retrospective analysis was approved by the local Ethics Committee (permit 142/20 S-KH). The administration

of F-18-flubrobenguane complied with The German Medicinal Products Act, AMG §13 2b, and the responsible regulatory body (Government of Oberbayern).

Patient Population and Imaging Protocol

23 patients with clinical suspicion or history of pheochromocytoma or paraganglioma underwent whole body (head to mid-thigh) PET/CT (Biograph mCT) or PET/MR imaging (Biograph mMR) between August 2016 and November 2018 (Tabl. 1). Fifteen patients underwent at least one other imaging modality prior to F-18-flubrobenguane PET (CT = 8, MRI = 9), including four patients who had received I-123-MIBG-SPECT/CT in their medical history. In total, 26 PET scans (24 PET/CTs, 2 PET/MRI (3 patients were scanned twice)) were performed after the injection of mean 256 ± 33 MBq [range 183-307]. PET acquisition was started after 63 ± 24 minutes [range 43-143 min.]. In PET/CT a diagnostic CT scan in portal venous phase was performed (Imeron 300 at 1.5 ml/kg body weight). In PET/MRI the following sequences were acquired: T1 VIBE Dixon sequence (for attenuation correction purposes), axial and coronal T2 haste (skull to mid-thigh), axial DWI, axial T1 VIBE with contrast dynamics, axial T1 in-/opposed phase, axial T1 VIBE fs (all upper abdomen). For contrast enhanced MR imaging 0.2 ml/kg body weight of DOTAREM® 0.5 mmol/ml were injected.

Quantitative and Qualitative Image Analysis

Biodistribution of F-18-flubrobenguane was quantified by mean and maximum values of the standardized uptake value corrected for body weight (SUV_{mean} and SUV_{max}) (19). Spherical volume-of-interests with 1 cm diameter (salivary glands, thyroid, myocardium, stomach, pancreas) and 2 cm diameter (bladder, liver, spleen, kidney, muscle, aortic lumen, lungs) were placed inside the organs' parenchyma. Uptake of tumor lesions (SUV_{mean} and SUV_{max}) was measured by circular, three-dimensional regions of interest at a 40 % isocontour around the lesions using Syngo.Via software (Siemens Healthcare).

Imaging data of the hybrid PET/CT or combined PET/MRI were read separately against the respective cross-section imaging dataset only by a dual board-certified radiologist and nuclear medicine physician. Lesion size and number were reported and the diagnostic certainty for positive lesions was rated using the categories “possible”, “probable” or “consistent with”.

Additionally, in the four subjects who underwent both I-123-MIBG SPECT/CT and F-18-flubrobenguane PET/CT, imaging datasets were compared visually for divergent findings.

Histopathology

Thirteen patients (13/23, 57%) underwent surgery and subsequent histopathological analysis of the tumor lesions. 11 of those had a positive finding (11/13, 85%): 2 patients had proven paraganglioma (2/11: 18%) and 9 patients had a pheochromocytoma (9/11: 82%). In 2 patients (2/13, 15%) an adrenal adenoma was diagnosed.

Statistics

Data is reported as mean \pm standard error of the mean (SEM) and all statistical analysis were performed with GraphPad Prism 8.4.2 (GraphPad Software, San Diego, USA). To compare groups the student t-test or ANOVA if more than two groups were compared and data was normally distributed were applied. Mann-Whitney test was performed for nonparametric data. Differences were considered as statistically significant with p-values <0.05 .

RESULTS

Quantitative Analysis of Biodistribution and Tumor Lesions

F-18-flubrobenguane shows stable and reproducible biodistribution in healthy organs. Highest uptakes (SUV_{mean}) were observed in thyroid glands (22.5 ± 1.6), pancreas (9.5 ± 0.7) and kidneys (8.8 ± 0.7), the latter due to the excretion pathway of the radiotracer. Accordingly, high uptake in the urinary bladder was observed

(8.7 ± 1.5). Lowest uptake (SUV_{mean}) could be observed in lungs (1.85 ± 0.13), muscles (0.7 ± 0.04) and bloodpool (0.65 ± 0.03).

Lesions suspicious for pheochromocytoma and paraganglioma demonstrated very intense tracer uptake (SUV_{mean} 10.1 ± 1.1) which was significantly higher than uptake in liver parenchyma and healthy adrenal glands (Figs. 1 and 2A, 4.9 ± 0.3 and 3.7 ± 0.24 , respectively; each $p < 0.0001$; SUV_{max} : 16.8 ± 1.7 vs. 6.7 ± 0.4 vs 12.2 ± 0.95 , $p < 0.01$) (Fig. 2). Uptake in pheochromocytoma and paraganglioma was relatively similar (SUV_{mean} : 11.9 ± 2.0 vs 9.9 ± 1.5 , $p = 0.44$; SUV_{max} : 19.0 ± 3.0 vs 16.8 ± 2.1 , $p = 0.55$). Also when pheochromocytoma and paraganglioma were evaluated separately, a significantly higher tracer uptake compared to healthy adrenal glands was present (SUV_{mean} : 11.9 ± 2.0 vs 9.9 ± 1.5 vs 3.7 ± 0.2 , $p < 0.01$; SUV_{max} : 19.0 ± 3.0 vs 16.8 ± 2.1 vs 12.2 ± 0.95 , $p < 0.05$) (Fig. 2.).

Lesion Detection and Certainty

In total, 47 lesions were detected on hybrid PET/CT or PET/MRI reading. No statistically significant difference in number of lesions or lesion size was present. Still, a clearly higher number of lesions (1.8 ± 0.4 vs 1.1 ± 0.2 , $p = 0.24$) was reported in hybrid reads compared to CT/MRI reads (Fig. 3A). Especially, a smaller mean lesion size was reported by F-18-flubrobenguane PET/CT or MRI (1.7 ± 0.2 cm vs 2.2 ± 0.3 cm, $p = 0.10$) (Fig. 3B). In addition, diagnostic certainty for positive lesions was superior for F-18-Flubrobenguane hybrid imaging with 62.5% of lesions rated as “consistent with”, 25.0% rated as “probable” and 12.5% rated as possible compared to 35.5%, 38.7% and 25.8%, respectively, in CT/MRI only (Fig. 3C). Interestingly, out of the 47 lesions detected in total, 31 (66%) were found both in the cross-sectional imaging datasets only and the PET hybrid read, while 16 (34%) were found in PET hybrid imaging only. None of the lesions was only described in the cross-sectional imaging read. Of note, 61% (14/23) of the 23 (23/47, 49%) lesions smaller than 1 cm were found on hybrid imaging only, while 92% (22/24) of the lesions larger than 1 cm were also detected in the cross-sectional imaging read (Fig. 3D).

Case Examples

Figure 4 depicts two cases of F-18-flubrobenguane PET/CT images. First, a 50 year old male was referred due to a unclear lesion on conventional imaging in the left adrenal gland and a history of hypertension. F-18-flubrobenguane PET/CT did only show mild tracer uptake and surgical resection diagnosed an aldosterone-producing adenoma (Fig. 4A). In another case of a 57-year old male with elevated metanephrine plasma concentrations, a contrast enhancing, centrally hypodense lesion with intense F-18-flubrobenguane was detected in the right adrenal gland suspicious for pheochromocytoma. Subsequent surgical resection and histopathology verified imaging results. Note correspondence between the necrotic area within the tumor which shows no tracer-uptake and intense tracer uptake in the vital surrounding area (Fig. 4B). In our cohort only two individuals were diagnosed with an adrenal adenoma after surgical resection, the adenomas and the healthy adrenal glands of these patients did show similar SUV_{mean} (Supplemental Fig. 1).

In the third case a 38-year old patient with recurrent pheochromocytoma and status post multiple resections received a I-123-MIBG SPECT/CT due to suspected recurrence (Supplemental Fig. 2). The scan revealed suspicious lesions paravertebral close to the left kidney. In a follow-up scan with F-18-flubrobenguane PET/CT imaging 6 months later two small sized lesions with intense F-18-flubrobenguane uptake could be identified in the pelvis which were not detectable on I-123-MIBG SPECT/CT. In another follow-up F-18 flubrobenguane PET/CT 14 months after the SPECT/CT, lesions were still detectable and an overall stable disease was reported. Since a stable condition was previously reported over several years by means of annual I-123 MIBG SPECT/CT examinations, a progressive disease appears very unlikely and the reason for the detection of additional lesions most likely lies in the superiority of the F-18-flubrobenguane PET over the I-123 SPECT. It must be noted, however, that this single case description does not allow general conclusions on a comparison of the two tracers and imaging modalities.

DISCUSSION

In the present retrospective study, a novel F-18 labeled PET radiotracer targeting the norepinephrine transporter, F-18-flubrobenguane, was evaluated in 23 patients with clinical suspicion or history of pheochromocytoma or paraganglioma. Results demonstrate a favorable biodistribution with intense tracer uptake in pheochromocytoma and paraganglioma clearly above normal adrenal glands and surrounding liver tissue. Furthermore, it was demonstrated that hybrid F-18-flubrobenguane PET/CT or PET/MRI lead to a higher diagnostic certainty compared to morphological imaging with CT or MRI alone. Particularly lesions smaller than 1 cm were more often found to be suspicious for pheochromocytoma and paraganglioma with F-18-flubrobenguane PET compared to morphological imaging alone.

While already various PET tracers are available for the assessment of pheochromocytomas or paragangliomas, such as C-11-hydroxyephedrine, F-18-fluoro-dopa, F-18-fluorodopamine or I-124 MIBG, these tracers have not found the way into clinical routine because of various disadvantages such as short half-life or complex radiosynthesis. Accordingly, in the clinical setting usually I-123-/I-131-MIBG SPECT/CT, F-18-FDG or somatostatin receptor targeted imaging (e.g. Ga-68-DOTATATE) are used, which all demonstrate a rather low sensitivity and/or specificity. Previously published data favors Ga-68-DOTATATE compared to F-18-FDG because of a higher lesion-to-background contrast and a similar detection rate as I123-MIBG SPECT/CT, however the somatostatin receptor is not a specific target of pheochromocytoma and paraganglioma (13,20,21).

Because of its' broad availability iodine-labelled MIBG is the most applied radiotracer for pheochromocytoma/paraganglioma SPECT/CT-imaging. MIBG is a guanethidine analog with structural similarities compared to nor-epinephrine (22) and is often used for imaging of adrenal neoplasms (especially pheochromocytoma/paraganglioma and neuroblastoma). For imaging purposes the radionuclide I-123 has shown advantages over I-131, being a lower radiation burden to the patient and superior image quality and a higher sensitivity and specificity (23–25). On the downside MIBG-SPECT/CT has lower image quality

with low tracer-to-background ratios, no quantitative imaging and often multiple acquisition time points are needed (4h and 24h p.i.), resulting in only limited patient comfort and compliance. Consequently, there is a (yet) unmet clinical need for feasible PET tracers not just for primary staging and diagnosis but for the assessment of therapy response and follow-up examinations as well.

In the last couple of years F-18-flubrobenguane (formerly known as LMI-1195) gained more and more attention especially for cardiac sympathetic innervation imaging and its application (mostly in small animals) has been thoroughly described (15–18,26–29). These findings underline the potential clinical application of this tracer. Further, first in vivo studies showed that F-18-flubrobenguane is a suitable PET tracer for pheochromocytoma in a MENX model and therefore interesting for clinical applications (16).

It is commonly known that PET imaging has multiple major advantages compared to I-123-/I-131-MIBG-SPECT with better imaging quality, faster acquisition at a single timepoint at a comparable effective dose and possibility of true quantification (17,30). With this in view, F-18-flubrobenguane combines both PET-imaging and a MIBG-analogue, which might allow a superior evaluation of therapy response or progressive disease on follow-up examinations to previous methods (31–33).

This work is the first to evaluate F-18-flubrobenguane as a diagnostic tool in patients with the suspicion of pheochromocytoma and paraganglioma. Due to the relatively small cohort of subjects, the scope of this work was not the evaluation of the diagnostic accuracy (e.g. sensitivity and specificity) of this new diagnostic modality but to assess its principle applicability in this patient population. Of note, all patients with histopathological proven pheochromocytoma or paraganglioma were judged positive on F-18-flubrobenguane-PET indicating high potential for further clinical assessment.

We were able to show that F-18-flubrobenguane is a suitable PET tracer in pheochromocytomas and paragangliomas with excellent imaging quality and a high tracer-to-background ratio. Tumor lesions demonstrated a significantly higher tracer uptake than healthy adrenal glands and liver parenchyma, making it easier for readers to discriminate pathological tracer uptake of the adrenal to the liver

parenchyma or contralateral normal adrenal gland. Additionally, our limited reader data hints that F-18-flubrobenguane PET hybrid imaging can be beneficial in detecting smaller tumor lesions with more certainty compared to conventional imaging. Of course, this needs to be validated in larger cohorts or even prospective trials.

Further studies are warranted to investigate the performance of F-18-flubrobenguane in larger clinical trials, particularly with a head-to-head comparison to I-123-MIBG-SPECT and conventional imaging like MRI and CT, which could result in a change in diagnostic management.

Limitations

There are several limitations of this retrospective analysis. First, we investigated a small and heterogeneous patient cohort, including patients with suspected or recurrent paraganglioma or pheochromocytoma. Further, only slightly more than half of the cohort histopathological validation was possible. In cases without histopathological results, no defined reference standard was available. This is an inherent problem of negative diagnostic test results and could be solved by follow-up examinations. Consequently we omitted calculation of sensitivity and specificity. Future - preferably prospective – studies need to investigate whether the F-18-flubrobenguane-PET really results in an additional value over established examinations such as CT, MRI or I-123 MIBG SPECT since this question cannot be answered conclusively in the present retrospective study using a clinical patient group in a real-life scenario.

CONCLUSION

The F-18-labeled catecholamine-analogue F-18-flubrobenguane represents a promising radiotracer for the detection and staging of pheochromocytomas and paragangliomas. F-18-flubrobenguane provides stable and reproducible biodistribution with high uptake in tumor lesions. The relatively fast acquisition time and excellent image quality on PET is advantageous for pheochromocytoma and paraganglioma staging and further applications in other tumor entities should be

investigated as well (e.g. neuroblastoma). Nonetheless, there have not been thorough comparisons of this novel tracer to other established diagnostic methods (e.g. I-123-/I-131-MIBG SPECT/CT, MRI), so its clinical benefits are still to be evaluated in larger clinical trials.

KEY POINTS

QUESTION: Is the novel sympathetic nerve imaging tracer F-18-flubrobenguane suitable for the evaluation of patients with suspected pheochromocytoma (PHEO) or paraganglioma (PGL)?

PERTINENT FINDINGS: In a patient group of 24 patients with suspected PHEO or PGL, a total of 47 lesions were detected and when comparing the hybrid F-18-flubrobenguane PET/CT examination with conventional imaging, more and smaller lesions were described without reaching statistical significance. A significantly higher tracer accumulation was found in PHEO or PGL compared to the healthy adrenal gland.

IMPLICATIONS FOR PATIENT CARE: F-18-flubrobenguane PET is a promising imaging modality in patients with suspected PHEO and PGL and should be investigated in larger studies.

REFERENCES

1. Lenders JWM, Eisenhofer G, Mannelli M, Pacak K. Pheochromocytoma. *Lancet (London, England)*. 2005;366:665-75.
2. Lenders JWM, Duh Q-Y, Eisenhofer G, et al. Pheochromocytoma and paraganglioma: an endocrine society clinical practice guideline. *J Clin Endocrinol Metab*. 2014;99:1915-42.
3. Modigliani E, Vasen HM, Raue K, et al. Pheochromocytoma in multiple endocrine neoplasia type 2: European study. The Euromen Study Group. *J Intern Med*. 1995;238:363-7.
4. Lonser RR, Glenn GM, Walther M, et al. von Hippel-Lindau disease. *Lancet (London, England)*. 2003;361:2059-67.
5. Gruber LM, Erickson D, Babovic-Vuksanovic D, Thompson GB, Young WF, Bancos I. Pheochromocytoma and paraganglioma in patients with neurofibromatosis type 1. *Clin Endocrinol (Oxf)*. 2017;86:141-149.
6. Waguespack SG, Rich T, Grubbs E, et al. A current review of the etiology, diagnosis, and treatment of pediatric pheochromocytoma and paraganglioma. *J Clin Endocrinol Metab*. 2010;95:2023-37.
7. Edström Elder E, Hjelm Skog A-L, Höög A, Hamberger B. The management of benign and malignant pheochromocytoma and abdominal paraganglioma. *Eur J Surg Oncol*. 2003;29:278-83.
8. Lloyd R, Osamura R, Kloppel G, Rosai J. WHO classification of tumours: pathology and genetics of tumours of endocrine organs: 4th Edition. 2017;10:179-206.
9. Welch TJ, Sheedy PF, van Heerden JA, Sheps SG, Hattery RR, Stephens DH. Pheochromocytoma: Value of computed tomography. *Radiology*. 1983;148:501-503.
10. Ganguly A, Henry DP, Yune HY, et al. Diagnosis and localization of pheochromocytoma. Detection by measurement of urinary norepinephrine excretion during sleep, plasma norepinephrine concentration and computerized axial tomography [CT-scan]. *Am J Med*. 1979;67:21-26.
11. Hicks RJ, Hofman MS. Is there still a role for SPECT-CT in oncology in the PET-CT era? *Nat Rev Clin Oncol*. 2012;9:712-20.
12. Pandit-Taskar N, Modak S. Norepinephrine transporter as a target for imaging and therapy. *J Nucl Med*. 2017;58:39S-53S.
13. Jing H, Li F, Wang L, et al. Comparison of the 68Ga-DOTATATA PET/CT, FDG PET/CT, and MIBG SPECT/CT in the evaluation of suspected primary pheochromocytomas and paragangliomas. *Clin Nucl Med*. 2017;42:525-529.
14. Green M, Lowe J, Kadirvel M, et al. Radiosynthesis of no-carrier-added meta-[124I]iodobenzylguanidine for PET imaging of metastatic neuroblastoma. *J Radioanal Nucl Chem*. 2017;311:727-732.
15. Yu M, Bozek J, Lamoy M, et al. Evaluation of LMI1195, a novel 18F-labeled cardiac neuronal PET imaging agent, in cells and animal models. *Circ Cardiovasc Imaging*. 2011;4:435-43.
16. Gaertner FC, Wiedemann T, Yousefi BH, et al. Preclinical evaluation of

- 18F-LMI1195 for in vivo imaging of pheochromocytoma in the MENX tumor model. *J Nucl Med*. 2013;54:2111-7.
17. Sinusas AJ, Lazewatsky J, Brunetti J, et al. Biodistribution and radiation dosimetry of LMI1195: First-in-human study of a novel 18F-labeled tracer for imaging myocardial innervation. *J Nucl Med*. 2014;55:1445-1451.
 18. Zelt JGE, Mielniczuk LM, Orlandi C, et al. PET imaging of sympathetic innervation with [18F]Fluorobenguan vs [11C]mHED in a patient with ischemic cardiomyopathy. *J Nucl Cardiol*. 2019;26:2151-2153.
 19. Giesel F, Kratochwil C, Lindner T, et al. FAPI-PET/CT: biodistribution and preliminary dosimetry estimate of two DOTA-containing FAP-targeting agents in patients with various cancers. *J Nucl Med*. August 2018;jnumed.118.215913.
 20. Chang CA, Pattison DA, Tohill RW, et al. 68Ga-DOTATATE and 18F-FDG PET/CT in paraganglioma and pheochromocytoma: utility, patterns and heterogeneity. *Cancer Imaging*. 2016;16:22.
 21. Janssen I, Blanchet EM, Adams K, et al. Superiority of [68Ga]-DOTATATE PET/CT to other functional imaging modalities in the localization of SDHB-associated metastatic pheochromocytoma and paraganglioma. *Clin Cancer Res*. 2015;21:3888-3895.
 22. Chen CC, Carrasquillo JA. Molecular imaging of adrenal neoplasms. *J Surg Oncol*. 2012;106:532-542.
 23. Furuta N, Kiyota H, Yoshigoe F, Hasegawa N, Ohishi Y. Diagnosis of pheochromocytoma using [123I]-compared with [131I]-metaiodobenzylguanidine scintigraphy. *Int J Urol*. 1999;6:119-24.
 24. Mattsson S, Johansson L, Leide Svegborn S, et al. ICRP publication 128: Radiation dose to patients from radiopharmaceuticals: a compendium of current information related to frequently used substances. *Ann ICRP*. 2015;44:7-321.
 25. Van Der Horst-Schrivers ANA, Jager PL, Boezen HM, Schouten JP, Kema IP, Links TP. Iodine-123 metaiodobenzylguanidine scintigraphy in localising phaeochromocytomas - experience and meta-analysis. *Anticancer Res*. 2006;26:1599-1604.
 26. Yu M, Bozek J, Lamoy M, et al. LMI1195 PET imaging in evaluation of regional cardiac sympathetic denervation and its potential role in antiarrhythmic drug treatment. *Eur J Nucl Med Mol Imaging*. 2012;39:1910-9.
 27. Higuchi T, Yousefi BH, Kaiser F, et al. Assessment of the 18F-labeled PET tracer LMI1195 for imaging norepinephrine handling in rat hearts. *J Nucl Med*. 2013;54:1142-6.
 28. Yu M, Bozek J, Kagan M, et al. Cardiac retention of PET neuronal imaging agent LMI1195 in different species: impact of norepinephrine uptake-1 and -2 transporters. *Nucl Med Biol*. 2013;40:682-8.
 29. Werner RA, Rischpler C, Onthank D, et al. Retention kinetics of the 18F-Labeled sympathetic nerve PET tracer LMI1195: Comparison with 11C-Hydroxyephedrine and 123I-MIBG. *J Nucl Med*. 2015;56:1429-33.
 30. Radiation dose to patients from radiopharmaceuticals (addendum 2 to

- ICRP publication 53). *Ann ICRP*. 1998;28:1-126.
31. Rahmim A, Zaidi H. PET versus SPECT: strengths, limitations and challenges. *Nucl Med Commun*. 2008;29:193-207.
 32. Garcia E V. Physical attributes, limitations, and future potential for PET and SPECT. *J Nucl Cardiol*. 2012;19 Suppl 1:S19-29.
 33. Gholamrezanejhad A, Mirpour S, Mariani G. Future of nuclear medicine: SPECT versus PET. *J Nucl Med*. 2009;50:16N-18N.

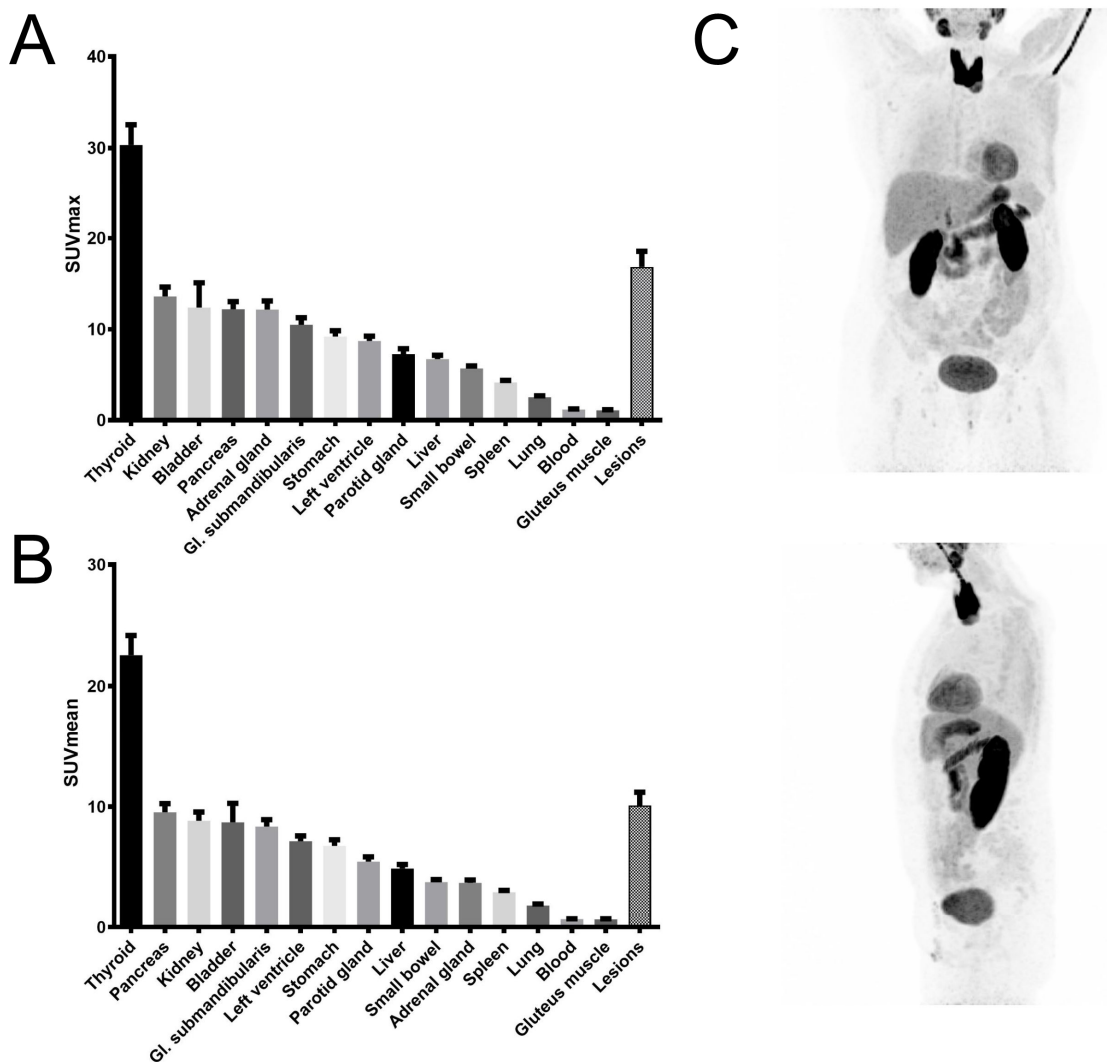


Fig. 1. Biodistribution of F-18-flubrobenguane in the respective organs (A) SUV_{max} (B) SUV_{mean}. Highest uptake (SUV_{max/mean}) can be observed in thyroid, pancreas and pheochromocytoma and paraganglioma lesions. Low uptake was observed in muscle, lung and bloodpool (aortic lumen). (C) shows a MIP of a negative PET scan.

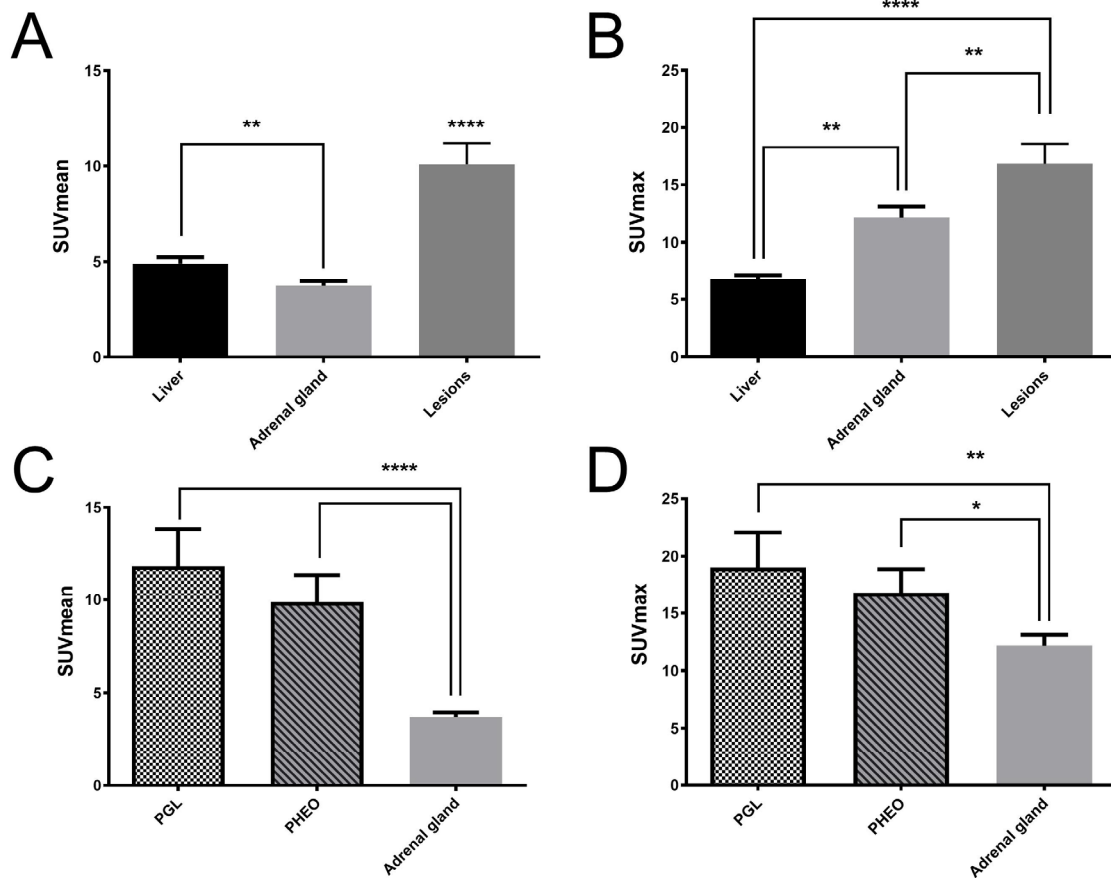


Fig. 2. SUVmax and SUVmean of tumorlesions, liver and adrenal glands compared.

All lesions, pheochromocytoma (PHEO) and paraganglioma (PGL), showed a significantly higher SUV_{mean} compared to liver parenchyma and adrenal glands **(A)** whereas SUV_{mean} of liver parenchyma was significantly higher than normal adrenal glands. SUV_{max} was significantly higher in lesions and healthy adrenal glands compared to liver parenchyma **(B)**. PGL and PHEO lesions show significantly higher uptake compared to healthy adrenal glands and liver. Uptake was significantly higher in PGL and PHEO, both for SUV_{mean} **(C)** and SUV_{max} **(D)**. (* $p < 0.05$; ** $p < 0.01$, **** $p < 0.0001$).

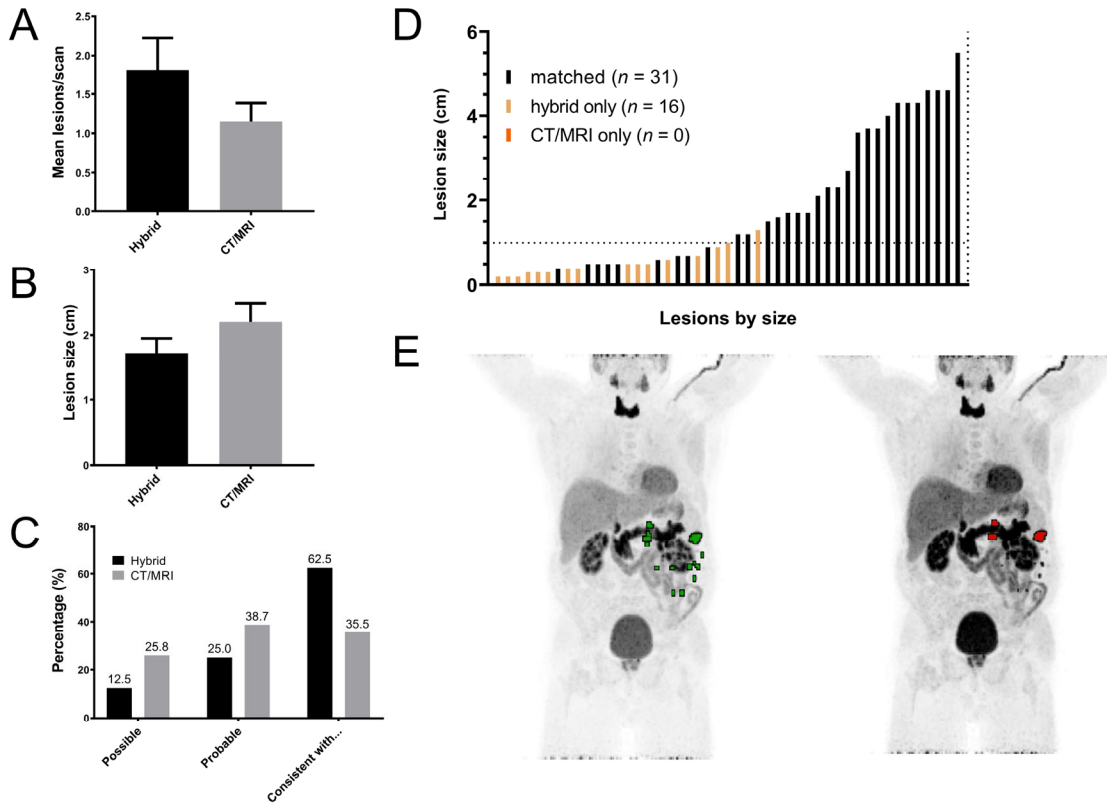


Fig. 3. Separate and combined reading of F-18-flubrobenguane PET and CT/MRI.

Lesion detection showed no significantly different number of lesions per scan (**A**) and lesion size in both reads (**B**). Lesion rating by reader certainty showed higher certainty in hybrid reads (**C**). In total, 47 lesions were detected. Most lesions were found in CT/MRI and hybrid (“matched” $n=31$) but no lesion was detected in CT/MRI only ($n=0$) but several lesions were detected only by PET hybrid imaging ($n=16$). An increased number of smaller lesions were detected by PET hybrid imaging (**D**). In (**E**) representative MIPs of a patient with multiple lesions are shown. The left MIP shows lesions reported in hybrid imaging (green) and in the right MIP lesions reported by CT/MRI reading only (red).

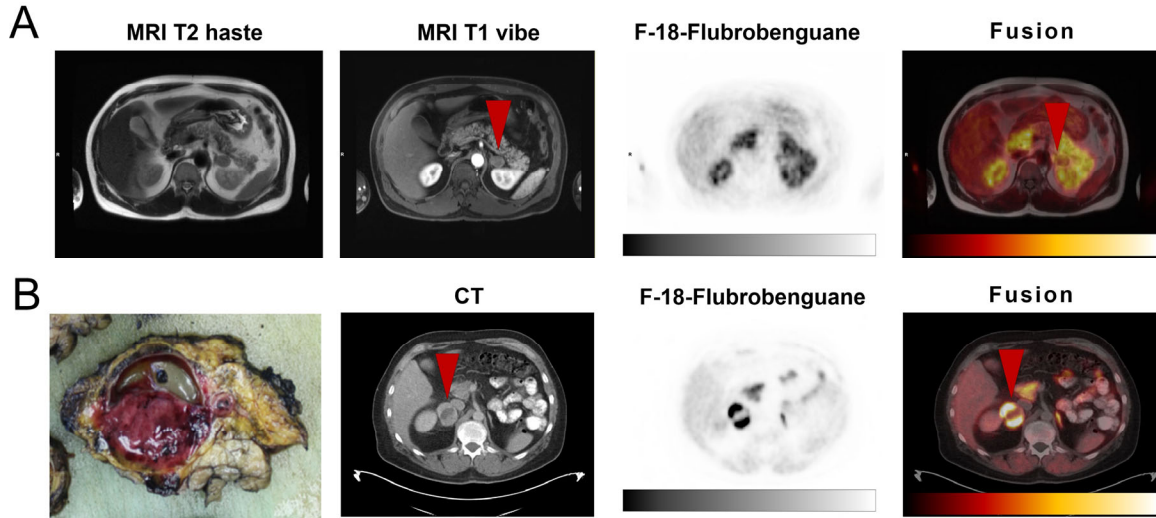


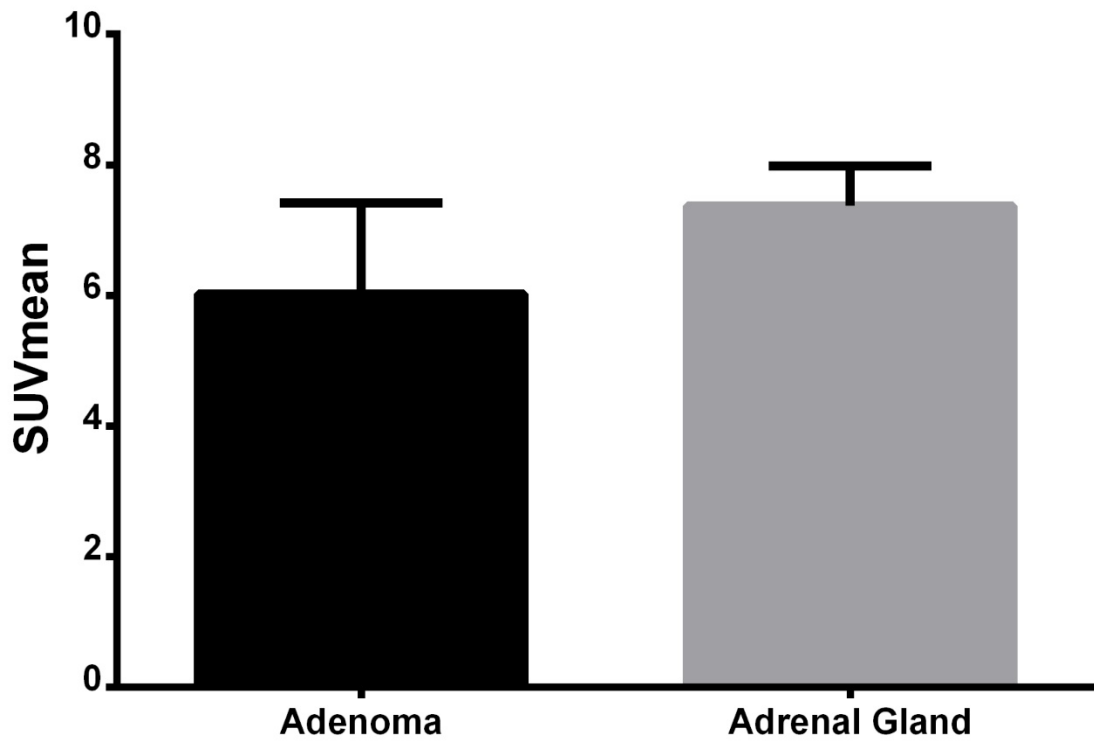
Fig. 4. Case examples of adrenal adenoma and pheochromocytoma. (A) shows the case of a 50 year old male with unclear hypertension and a suspected lesion in the left adrenal gland. F-18-flubrobenguane PET/CT did only show mild tracer uptake and surgical resection diagnosed a aldosterone-producing adenoma. (B) Case examples of a 50 year of 57-year old male with pathological elevated metanephrine plasma concentration. Pheochromocytoma could be detected in the right adrenal gland in F-18-flubrobenguane PET/CT with increased tracer uptake in lesions, but focal lack of uptake in the central necrotic tissue of the pheochromocytoma, which could be verified after surgical resection.

TABLES

Table 1. Patient characteristics and scan details. *suspicion of pheochromocytoma (PHEO paraganglioma (PGL) due to other morphological imaging modality. Patient no. 6, 11 and 19 underwent repetitive scans.

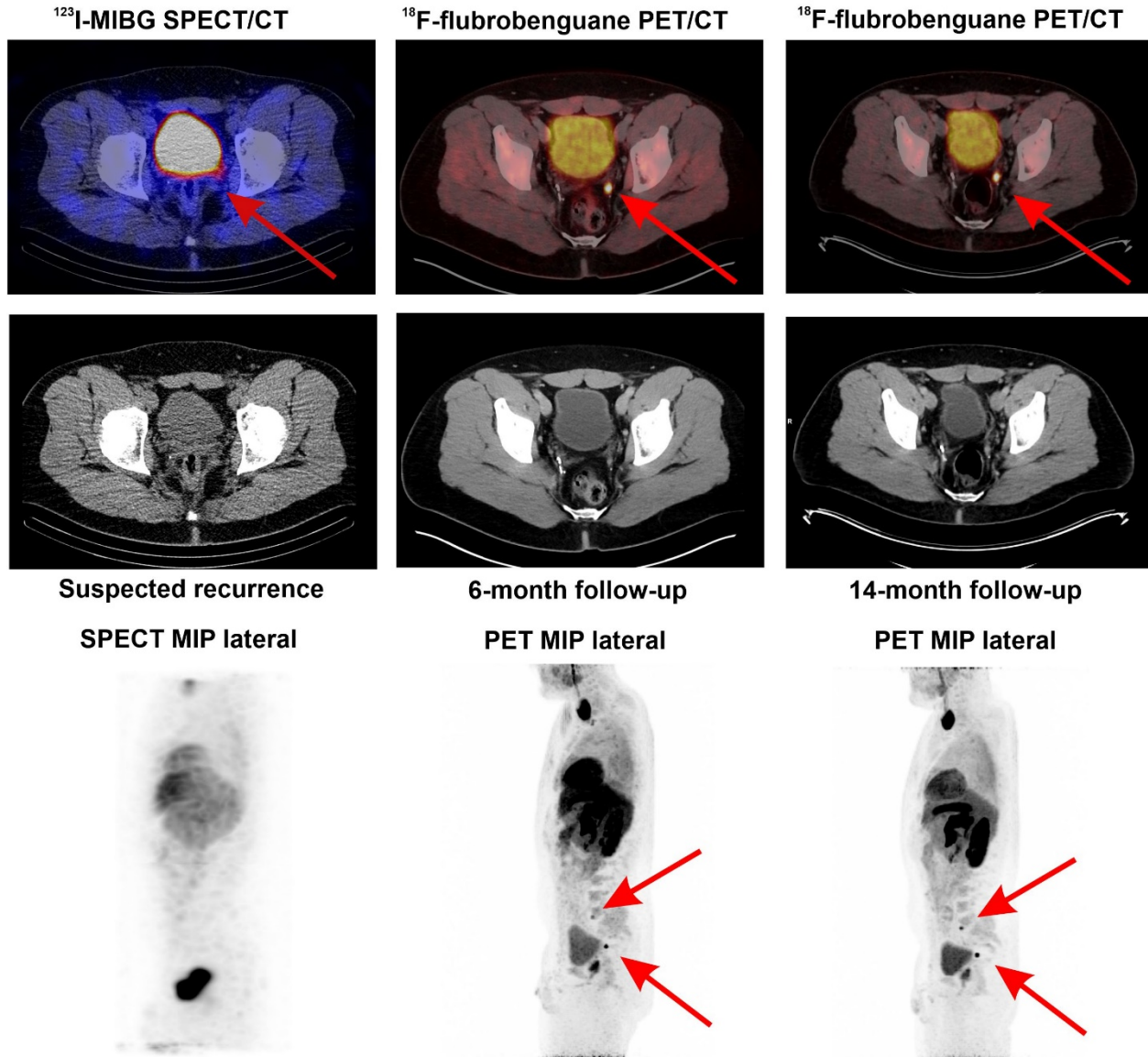
† patients with a histopathological result after surgery.

| Patient no. | Age | Activity [MBq] | Scan p.i. [min] | Scanner | Indication for scan | Imaging result | No. of lesions hybrid | No. of lesions CT/MRI |
|-------------|-----|----------------|-----------------|---------|-------------------------|-------------------|-----------------------|-----------------------|
| 1 | 57 | 291 | 43 | PET/CT | suspicion of PHEO* | primary PHEO † | 1 | 1 |
| 2 | 45 | 218 | 46 | PET/CT | suspicion of PHEO* | primary PHEO † | 1 | 1 |
| 3 | 71 | 253 | 81 | PET/CT | clinical suspicion | Normal | 0 | 0 |
| 4 | 62 | 183 | 45 | PET/CT | clinical suspicion | Normal | 0 | 0 |
| 5 | 57 | 251 | 56 | PET/CT | suspicion of PHEO* | primary PHEO † | 1 | 1 |
| 6 | 38 | 256 | 58 | PET/CT | PGL in history | recurrent PGL | 4 | 1 |
| 7 | 63 | 275 | 54 | PET/CT | suspicion of PHEO* | adrenal adenoma † | 1 | 1 |
| 8 | 55 | 290 | 54 | PET/CT | suspicion of PHEO* | primary PHEO † | 1 | 1 |
| 9 | 48 | 270 | 59 | PET/CT | suspicion of PHEO* | primary PHEO † | 1 | 1 |
| 10 | 63 | 271 | 52 | PET/CT | PHEO in history | recurrent PHEO | 9 | 2 |
| 11 | 67 | 227 | 57 | PET/CT | PHEO and PGL in history | recurrent PHEO | 1 | 1 |
| 12 | 68 | 262 | 81 | PET/CT | suspicion of PHEO* | primary PHEO † | 1 | 1 |
| 13 | 50 | 224 | 45 | PET/MRI | suspicion of PHEO* | adrenal adenoma † | 0 | 1 |
| 14 | 68 | 297 | 72 | PET/CT | suspicion of PHEO* | primary PHEO † | 1 | 1 |
| 15 | 48 | 302 | 73 | PET/CT | catecholamines in urine | Normal | 2 | 0 |
| 16 | 55 | 213 | 87 | PET/CT | suspicion of PGL* | primary PGL † | 1 | 1 |
| 17 | 77 | 237 | 143 | PET/CT | suspicion of PHEO* | primary PHEO | 1 | 1 |
| 18 | 41 | 245 | 45 | PET/CT | PGL in history | recurrent PGL | 3 | 1 |
| 19 | 62 | 254 | 97 | PET/CT | PGL in history | recurrent PGL † | 7 | 6 |
| 20 | 56 | 224 | 76 | PET/CT | suspicion of PHEO* | primary PHEO † | 1 | 1 |
| 21 | 51 | 228 | 55 | PET/MRI | suspicion of PHEO* | primary PHEO | 1 | 1 |
| 22 | 77 | 233 | 59 | PET/CT | suspicion of PHEO* | primary PHEO | 1 | 1 |
| 23 | 56 | 247 | 57 | PET/CT | suspicion of PHEO* | primary PHEO † | 1 | 1 |



Supplemental Fig. 1. Similar tracer uptake by adrenal adenoma and healthy adrenal glands.

The figure shows the SUVmean in a column graph of two patients with adrenal adenoma and the corresponding tracer uptake in their healthy adrenal gland.



Supplemental Fig. 2. Case example of 38-year old male with status post multiple paraganglioma resections.

An I-123-MIBG SPECT/CT was performed due to suspected recurrence and confirmed lesions paravertebral of the left kidney but no lesions in the pelvis. A follow up F-18-flubrobenguane PET/CT 6 months later unveiled a suspected lesion in the pelvis, which was stable in another follow-up by F-18-flubrobenguane PET/CT 14 months after SPECT/CT.